Thermal behaviour of citric acid and isomeric aconitic acids

D. Wyrzykowski · E. Hebanowska · G. Nowak-Wiczk ·
M. Makowski · L. Chmurzyński

Abstract Thermal decomposition of citric acid, *trans*- and *cis*-aconitic acid has been studied using the TG-MS, TG-FTIR and DSC techniques. The measurements were carried out in an argon atmosphere over a temperature range of 293–673 K. The influence of the acid structures and configurational geometry on stability of the transition products and pathways of thermal transformations of the studied compounds studied is discussed.

Keywords Citric acid · *Trans*-aconitic acid · *Cis*-aconitic acid · Thermal decomposition

Introduction

Citric acid, 2-hydroxypropane-1,2,3-tricarboxylic acid, is a natural compound occurring in human organisms and in plant and animal cells, generated during initial transformations in the Krebs cycle [1–3]. Since it is nontoxic, citric acid has found widespread application in the food industry as an antioxidant and preserving agent. It is also used in the metallurgical industry for cleaning metal surfaces prior to welding because it covers the metal surfaces with a protective coating. In the pharmaceutical industry, citric acid has been used as a stabilizer of active ingredients of preparations and as a flavouring additive in tablets.

Recently, interest in citric acid has grown owing to its use for the synthesis of nano-powders doped with rare earth metal ions, transition metals and others [4, 5]. In the Pechini method, the acid is used as a non-polymeric filler for size modification and porosity control of nano-powders. In this method, citric acid is removable by either heat treatment or thermal decomposition, without affecting the properties of a material [6–8].

Barbooti and Al-Sammerrai [9] reported on the thermal decomposition of citric acid. As stated, the decomposition is preceded by melting followed by dehydration and decarboxylation processes resulting in the formation of methyl maleic anhydride.

In order to acquire better insight into thermal transformations of citric acid, we have presented the broader characteristics of its thermal behaviour. To be able to do this, we have examined the intermediate dehydration products of the acid, *trans*-aconitic acid (*trans*-propene-1,2,3-tricarboxylic acid) and its *cis*-isomer, *cis*-propene-1,2,3-tricarboxylic acid. In our work the results of the TG-FTIR, TG-MS and DSC analyses of the three acids studied are presented.

Experimental

Materials

All reagents: citric acid, $C_6H_8O_7$, (ACS reagent, ≥99.5%), *trans*-aconitic acid, $C_6H_6O_6$, (≥98%) and *cis*-aconitic acid, $C_6H_6O_6$, (≥98%) were purchased from Aldrich Chemical Corp. and were used without further purification.

Methods

The TG-FTIR analyses in argon (Ar 5.0) were run on a Netzsch TG 209 apparatus coupled with a Bruker IFS 66 spectrometer (range 298–673 K, Al crucible with a small

D. Wyrzykowski (✉) · E. Hebanowska · G. Nowak-Wiczk ·
M. Makowski · L. Chmurzyński
Faculty of Chemistry, University of Gdańsk, Sobieskiego 18,
80-952, Gdańsk, Poland
e-mail: daro@chem.univ.gda.pl

central hole, sample mass 5–10 mg, heating rate 5, 10, 15 K min^{-1}, flow rate of the carrier gas 15 mL min^{-1}). The TG-DSC-MS measurements in argon (Ar 5.0) were run on a STA 449 F3 Jupiter® thermal analyzer (Netzsch) coupled with a QMS 403 C Aëolos® quadrupole mass spectrometer (range 308–673 K, Al crucible with a small central hole or open Al$_2$O$_3$ crucible, empty crucible as a reference, sample mass 5–10 mg, heating rate 5, 10, 15 K min^{-1}, flow rate of the carrier gas 20 mL min^{-1}). The DSC measurements were carried out in a model DSC 204 Netzsch calorimeter (range 298–673 K, Al crucible with a small central hole, empty Al crucible as a reference, sample mass 5–10 mg, heating rate 2, 5, 10 K min^{-1}, flow rate of the carrier gas 20 mL min^{-1}).
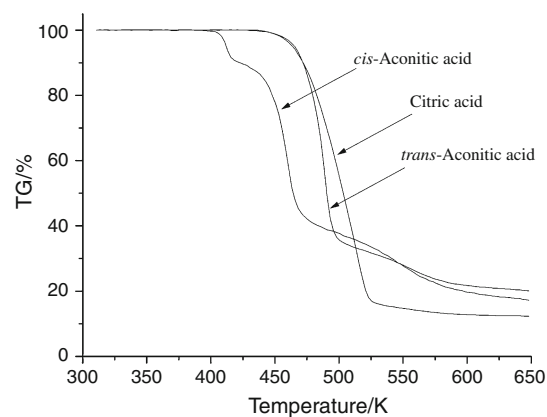
The DFT (density functional theory) method [10] with the B3LYP (Becke three-parameter hybrid exchange functional and the non-local correlation functional of Lee, Yang and Parr) functional [11, 12] and the 6-31+G** basis set [13] were used to optimize the structures of the systems studied. Geometries of isolated fragments were fully optimized without symmetry constraints. At the energy minima (with real frequencies) of a particular species, the energy parameters of isomerization process of *cis*-aconitic anhydride into *trans*-aconitic anhydride were calculated at 450 K using the same level of theory. The *G* values included changes at the zero-point energy (ZPE) and thermal corrections (vibrational, rotational and translational) to the enthalpy (*H*) and entropy (*S*). All calculations were performed using the Gaussian 03 program [14].
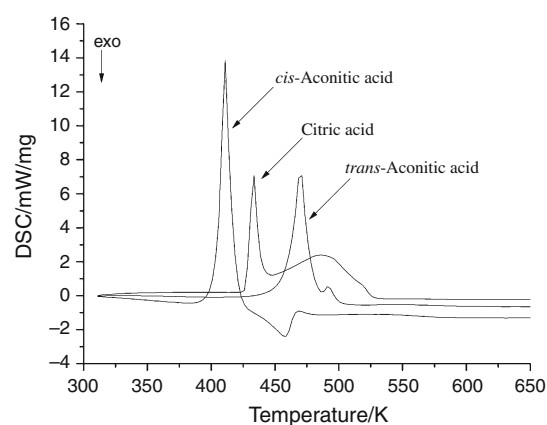
Results and discussion

The TG and DSC curves of the compounds recorded at a heating rate of 10 K min^{-1} in Al crucible are shown in Figs 1 and 2. The onset and the end decomposition temperature of citric acid, *trans*-aconitic acid and *cis*-aconitic acid determined by extrapolation are collected in Table 1. As seen, citric and *trans*-aconitic acid exhibit a comparable thermal stability in contrast to *cis*-aconitic acid whose decomposition point is 60–70 K lower than that of the remaining compounds.

Decomposition of citric acid is preceded by its melting. The melting point was determined by DSC measurements and equals 433.9 ± 0.2 K (average of eleven results ± standard error).

The shape of the TG curves of citric acid suggests that a single-step process occurs. However, in the DSC curve, over the temperature range covering that step, there is a broad endothermic peak with two non-symmetric inflexions indicating a complex decomposition process. Extremal peak temperatures and enthalpy changes for particular

Fig. 1 TG curves of thermal decomposition of citric acid, *trans*-aconitic acid and *cis*-aconitic acid in argon, $\beta = 10$ K min^{-1}

Fig. 2 DSC curves of thermal decomposition of citric acid, *trans*-aconitic acid and *cis*-aconitic acid in argon, $\beta = 10$ K min^{-1}

Table 1 The onset and the end decomposition temperature of citric acid, *trans*-aconitic acid and *cis*-aconitic acid in argon, $\beta = 5$, 10 and 15 K min^{-1}

Compound	5/K min^{-1}		10/K min^{-1}		15/K min^{-1}	
	T_{onset}	T_{end}	T_{onset}	T_{end}	T_{onset}	T_{end}
Citric acid	475.8	521.0	485.3	534.3	495.3	544
trans-Aconitic acid	477.3	504.4	488.1	518.7	501.7	526.7
cis-Aconitic acid	404.9	420.2	415.1	430.8	422.0	441.1
	447.5	466.2	461.1	478.9	472.1	485.9
	527.2	577.9	541.5	600.0	550.4	613.4

energetic effects accompanying heating of the compounds are shown on Table 2.

The inflexions in the DSC peak are probably due to overlapping of endothermic effects associated with decomposition of intermediate products formed when heating the sample (Fig. 2). Citric acid has been known to form thermodynamically stable complexes with various

Table 2 Temperature and enthalpy changes for physicochemical transformations of citric acid, *trans*-aconitic acid and *cis*-aconitic acid in argon, $\beta = 10$ K min^{-1}

Compound	T_p/K	ΔH/kJ mol^{-1}
Citric acid	433.0	40.15
	433–794.2	144.94
trans-Aconitic acid	471.4	87.77
	496.5	6.06
cis-Aconitic acid	407.7	86.55
	458.4	−23.61

T_p peak temperature, temperature at which a maximum of the thermal effect emerges

metal ions, including Al^{3+}, in which it occurs as a tridentate ligand [15, 16]. For this reason, to eliminate a catalytic influence of the aluminium crucible on thermal transformations of the acid, including the shape of the DSC curve, the experiment was performed in a corundum (Al$_2$O$_3$) crucible. In this case, the inflexions in the DSC curve also emerged, this indicating a multi-step course in the decomposition of the acid. Accordingly, examination of both the TG and DSC curves shows unambiguously that the decomposition of the acid under comparable conditions cannot be regarded as a single-step process.

The *trans*-aconitic acid does not melt before decomposition. Its first step ending around 510 K is characterized by two endothermic events in the DSC curve. They are indicative of a complex process in spite of a single step-like shape of the TG trace. The rate of the first step in the decomposition of the acid is faster than the corresponding one of citric acid over an analogous temperature range. For comparison, maximum mass loss rates determined from the DTG curves, at a heating rate of 10 K min^{-1} in Al crucibles with a small central hole, are 18 at 513 K and 40%/min at 489 K for citric and *trans*-aconitic acid, respectively.

Geometric configuration of the aconitic acid has a fundamental influence on the course of its decomposition. The *cis*-isomer is markedly less thermally stable than its *trans* counterpart. During the first step, the former loses one molecule of water to form *cis*-aconitic anhydride. This is demonstrated by a 9.8% mass loss (in TG curve) close to 10.3% as calculated for the loss of one water molecule, as well as by IR bands over the ranges 4000–3500 and 1750–1400 cm^{-1} assignable to water vapour. The dehydration step was further supported by ionic current intensities at m/z = 17 and 18, recorded over the temperature range studied.

The relatively thermally stable *cis*-aconitic anhydride undergoes subsequent decomposition. Unlike energetic effects accompanying thermal transformations of the remaining compounds, the second step of the decomposition

of the acid is exothermic (cf. DSC curve, Fig. 2). The exothermic reaction is probably due to conformational *cis*-aconitic anhydride → *trans*-aconitic anhydride transformation. This overweighing in excess endothermic effects of its further transformations.
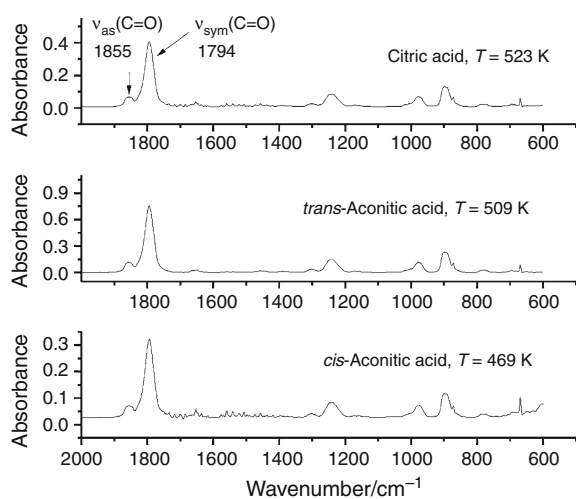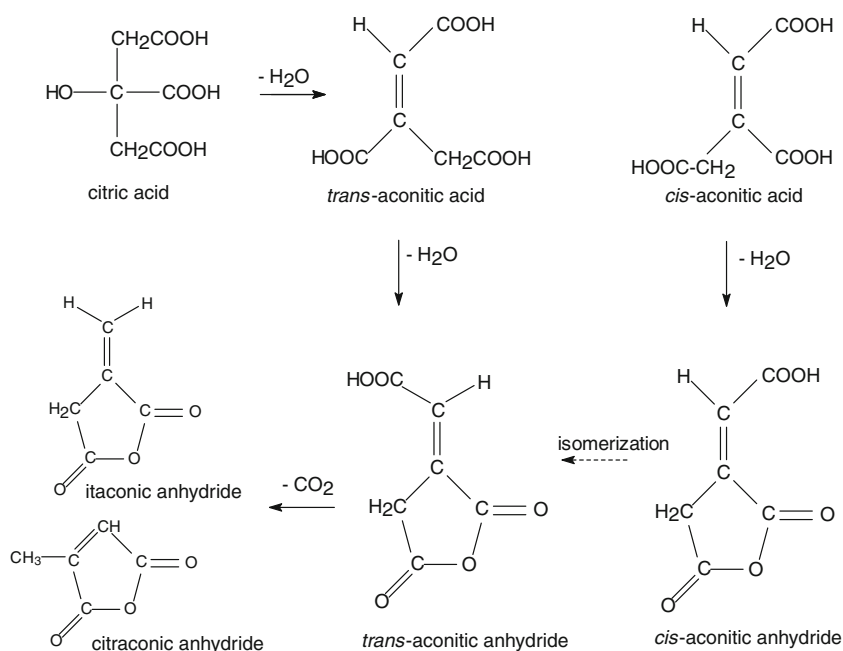
These assumptions have subsequently been verified by the change of isomerization enthalpy, $\Delta H_{isom.}$, calculated using the DFT method. Its value for the conversion *cis*-aconitic anhydride → *trans*-aconitic anhydride is $\Delta H_{isom.} = H_{trans} - H_{cis} = -30.66$ kJ mol^{-1}, where H_{trans} and H_{cis} denote enthalpies of the *trans*- and *cis*-isomers, respectively. The calculated free energy change, $\Delta G_{isom.}$, for the isomerization reaction is -27.48 kJ mol^{-1}.

The most probable thermal transformation pattern of the compounds studied is presented in Scheme 1. Decomposition of the compounds is a complex process leading through dehydration and decarboxylation reactions to different intermediate products. Due to similar structural features of the intermediate products, their identification is fairly difficult. The analysis of the volatiles using mass spectrometry revealed ions at m/z 39 and 68 in each case. However, they are characteristic of both the itaconic and citraconic anhydride. On the other hand, the IR spectra reveal that the decomposition of all the compounds studied affords identical products as demonstrated by bands at 1855 and 1794 cm^{-1} in the spectra of the volatiles, which are characteristic of cyclic acid anhydrides (Fig. 3). This, in turn, suggests that one of the final decomposition products is itaconic and/or citraconic anhydride.

In the MS spectra of the volatiles of all the samples studied, a ion with m/z = 112 is present which is likely to be a molecular ion of either itaconic or citraconic anhydride. This conclusion seems to be correct, although the two anhydrides cannot be distinguished from each other under the conditions of the measurement.

In order to acquire a better knowledge of the thermal transformations of the compounds, kinetic characteristics of their decomposition would be needed. In view of the complexity of the process, determination of the mechanism and kinetics of the reactions using the techniques mentioned in our paper so far would be fairly difficult if not impossible. The reasons for this are the following (i) models describing the kinetics of the decomposition processes refer to single-step reactions. Consequently, attempts to fit a kinetic model using numerical methods that assume the least standard deviations as a criterion, in the case of complex processes, result in a description incompatible with reality; (ii) attempts to determine kinetic parameters of a reaction, i.e. activation energy, E_a, or exponent in the Arrhenius equation (the Friedman or Ozawa–Flynn–Wall methods) would be charged with a huge error and their numerical values would not have a physical meaning. These reasons could explain discrepancies among the magnitudes of

Scheme 1 Thermal transformations of citric acid, *trans*-aconitic acid and *cis*-aconitic acid

Conclusions

This article presents the thermal properties of citric acid, cis-aconitic acid and trans-aconitic acid determined in a neutral atmosphere (Ar) under different velocities of sample heating. The analysis of the DSC curves shows that only decomposition of citric acid is proceeded by the melting of the sample. The lowest thermal stability is exhibited by cis-aconitic acid undergoing dehydration at the first stage of decomposition, which leads to the formation of cis-aconitic anhydride. The presence of the exothermic peak on the DSC curve suggests that cis-aconitic anhydride then undergoes isomerisation into trans-aconitic anhydride. In view of the lack of exothermic effects on the DSC curves of citric acid and trans-aconitic acid, it can be assumed that thermal transformations of both acids lead directly to the formation of trans-aconitic anhydride. The use of hyphenated techniques, i.e. TG-FTIR and TG-MS enabled a first time identification trial of the gaseous products resulting from decomposition of the acids studied. The analysis of the IR and MS spectra shows that the analyzed compounds undergo dehydration and decarboxylation leading to the formation of citraconic anhydride or itaconic anhydride or the mixture of both isomers regardless of the initial compound. In view of small differences in the structure of both compounds, it is not easy to identify any of the compounds on the basis of the obtained IR and MS spectra.

Fig. 3 IR spectra of the volatile products of the thermal decomposition of citric acid (523 K), *trans*-aconitic acid (509 K) and *cis*-aconitic acid (469 K) in argon

activation energy reported in the literature for a particular compound when the process runs through a number of steps [9, 17]. The discrepancies arise from the fact that E_a determined for multi-step processes refers to different elementary events depending on the extent of the reaction; (iii) for the dehydration reactions, which are usually reversible, the kinetics of decomposition depends on the partial pressure of water vapour over the sample being heated. For this reason, any description of the dehydration kinetics in the absence of a parallel measurement of the partial pressure variations in the oven seems to be inaccurate. This is because it is impossible to define the physical conditions of the measurement.

and the Informatics Computer Centre of the Metropolitan Academic Network (TASK, Gdańsk).

References

1. Beinert H, Kennedy MC. Engineering of protein bound iron-sulfur clusters. A tool for the study of protein and cluster chemistry and mechanism of iron-sulfur enzymes. Eur J Biochem. 1989;186:5–15.
2. Martin RB. Citrate binding of Al^{3+} and Fe^{3+}. J Inorg Biochem. 1989;28:181–7.
3. Lippard SJ. Principles of bioinorganic chemistry. Mill Valley: University Science Books; 1994. p. 352.
4. Cushing BL, Kolesnichenko VL, O'Connor CJ. Recent advances in the liquid-phase syntheses of inorganic nanoparticles. Chem Rev. 2004;104:3893–946.
5. Matraszek A, Szczygieł I. Modified Pechini synthesis of $Na_3Ce(PO_4)_2$ and thermochemistry of its phase transition. J Therm Anal Calorim. 2008;93:689–92.
6. da Silva MFP, de Souza Carvalho FM, da Silva Martins T, de Abreu Fantini MC, Isolani PC. The role of citrate precursors on the morphology of lanthanide oxides obtained by thermal decomposition. J Therm Anal Calorim. 2010;99:385–90.
7. Chai Y-L, Chang Y-S, Chen G-J, Hsiao Y-J. The effects of heat-treatment on the structure evolution and crystallinity of $ZnTiO_3$ nano-crystals prepared by Pechini process. Mater Res Bull. 2008;43:1066–73.
8. Hardy A, Van Werde K, Vanhoyland G, Van Bael MK, Mullens J, Van Poucke LC. Study of the decomposition of an aqueous metal-chelate gel precursor for $(Bi, La)4Ti_3O_{12}$ by means of TGA-FTIR TGA-MS and HT-DRIFT. Thermochim Acta. 2003;397:143–53.
9. Barbooti MM, Al-Sammerrai A. Thermal decomposition of citric acid. Thermochim Acta. 1986;98:119–26.
10. Par RG, Yang W. Density functional theory of atoms and molecules. New York: Oxford University Press; 1989.
11. Becke AD. Density-functional thermochemistry. III. The role of exact exchange. J Chem Phys. 1993;98:5648–52.
12. Lee C, Yang W. Development of the Colle-Salvetti correlation-energy formula into a functional of the electron density. Phys Rev. 1988;B37:785–9.
13. Jensen F. Introduction to computational chemistry. Chichester: Wiley; 1999.
14. Frisch MJ, et al. Gaussian 03, Revision C.02. Gaussian, Inc., Wallingford; 2004.
15. Matzapetakis M, Raptopoulou CP, Terzis A, Lakatos A, Kiss T, Salifoglou A. Synthesis, structural characterization, and solution behavior of the first mononuclear, aqueous aluminum citrate complex. Inorg Chem. 1999;38:618–9.
16. Wyrzykowski D, Chmurzyński L. Thermodynamics of citrate complexation with Mn^{2+}, Co^{2+}, Ni^{2+} and Zn^{2+} ions. J Therm Anal Calorim. 2009. doi:10.1007/s10973-009-0523-4.
17. Dollimore D, O'Connell C. A comparison of the thermal decomposition of preservatives, using thermogravimetry and rising temperature kinetics. Thermochim Acta. 1998;324:33–48.